

# Imaging findings of cerebral fat embolism syndrome: a case report

Journal of International Medical Research  
48(9) 1–6

© The Author(s) 2020

Article reuse guidelines:

[sagepub.com/journals-permissions](http://sagepub.com/journals-permissions)

DOI: 10.1177/0300060520950559

[journals.sagepub.com/home/imr](http://journals.sagepub.com/home/imr)



Yali Wang\* , Zihua Si\*, Jingzhe Han  and Shuangqing Cao

## Abstract

Cerebral fat embolism (CFE) syndrome is relatively rare in clinical practice. Currently, there is no uniform standard of magnetic resonance imaging for the diagnosis of the disease. In this report, we present head computed tomography and magnetic resonance images (T2-weighted images, fluid-attenuated inversion recovery images, diffusion-weighted images, and susceptibility-weighted images) in a case of CFE. This report explains the imaging characteristics of CFE and improves the clinician's understanding of this disease and its etiology.

## Keywords

Cerebral fat embolism, magnetic resonance imaging, diagnosis, fluid-attenuated inversion recovery, T2-weighted images, diffusion-weighted images, susceptibility-weighted images, case report

Date received: 27 March 2020; accepted: 27 July 2020

## Introduction

Cerebral fat embolism (CFE) syndrome is rarely observed in clinical practice. There is currently no uniform standard for the diagnosis of this disease. It is mainly diagnosed based on a patient's symptoms, signs, and auxiliary examinations. Of these auxiliary examinations, the diagnostic value of magnetic resonance T2-weighted imaging (T2WI), T2\*-weighted imaging (T2\*WI), fluid-attenuated inversion recovery (FLAIR) imaging, and diffusion-weighted imaging

(DWI) sequences for CFE has been reported.<sup>1</sup> However, these imaging techniques have limitations with respect to their

---

Department of Neurology, Harrison International Peace Hospital, Hengshui, Hebei, China

\*These authors contributed equally to this work.

### Corresponding author:

Shuangqing Cao, Department of Neurology, Harrison International Peace Hospital, 180 Renmin Dong Road, Taocheng District, Hengshui, Hebei 053000, China.  
Email: [hshycsq@163.com](mailto:hshycsq@163.com)



Creative Commons Non Commercial CC BY-NC: This article is distributed under the terms of the Creative

Commons Attribution-NonCommercial 4.0 License (<https://creativecommons.org/licenses/by-nc/4.0/>) which permits non-commercial use, reproduction and distribution of the work without further permission provided the original work is attributed as specified on the SAGE and Open Access pages (<https://us.sagepub.com/en-us/nam/open-access-at-sage>).

sensitivity and specificity. The pathogenesis of CFE mainly involves microemboli and microbleeds. Therefore, susceptibility-weighted imaging (SWI), which is sensitive to microbleeds, may also have important value for the diagnosis of CFE. This study reports the head computed tomography (CT) findings as well as the magnetic resonance T2WI, FLAIR, DWI, and SWI findings in a case of CFE. We then explain the imaging characteristics of CFE to improve clinicians' understanding of this disease and its etiology.

### **Case report**

An 82-year-old man was admitted to the hospital after 4 hours of progressive unconsciousness. The patient did not have any obvious "fall to the ground" episodes in the 4 hours before admission. His family members stated that he had no head injury or discomfort when standing. The patient subsequently developed breathing difficulties, chest tightness, and facial cyanosis. He developed gradual unconsciousness without limb twitches or incontinence. He was admitted to the Emergency Department of Harrison International Peace Hospital of Hengshui, Hebei, China, and blood gas analysis revealed pH 7.43, PCO<sub>2</sub> 30 mmHg, PO<sub>2</sub> 51 mmHg, base deficit -4.4 mmol/L, and SaO<sub>2</sub> 87%. He was admitted after emergency intubation and ventilator-assisted breathing. The patient had a history of tuberculosis 20 years earlier, a history of T12-L2 vertebral compression fracture for 10 years, and a history of arrhythmia/atrial fibrillation for 3 years. The results of his physical examination at the time of admission were as follows: temperature 37.7°C, P 136 times/minute, R 24 times/minute, blood pressure 104/57 mmHg, Glasgow coma scale (GCS) 4 points (E2-V1-M1), and SpO<sub>2</sub> 92%. Flake ecchymosis of the left elbow and the dorsal side of the left thigh were observed. He had low respiratory sounds in both lungs, but no rhonchus or moist rales were detected. His heart rate

was 154 beats/minute with an irregular rhythm. The first heart sound varied in intensity, and systolic blow-like murmurs at grade 3/6 were audible in the mitral and tricuspid auscultation areas. The abdomen was soft, and the liver and spleen were not revised. No edema was observed in the lower limbs. Examination of the nervous system revealed unconsciousness and a lack of cooperation in the examination. Eye movements were not able to cooperate to complete the examination. The pupils on both sides were equal, and the light reflex was observed. The tongue was unmovable. The patient's muscle strength in the limbs was difficult to examine; however, no activity was detected. Both Babinski signs were positive. A head and thoracic CT showed changes in white matter demyelination, brain atrophy, bronchitis, old pulmonary tuberculosis, and T12-L2 vertebral compression fractures. An electrocardiogram revealed arrhythmia/atrial fibrillation. The content of D-dimer was 66.9 mg/L, cardiac troponin I was 0.160 g/L, and brain natriuretic peptide was 3059 pg/mL. Cardiac ultrasound showed mitral regurgitation (a small amount), tricuspid regurgitation (a small amount), aortic regurgitation (a small amount), and pulmonary hypertension. The transcranial Doppler bubble test was negative. Head magnetic resonance imaging (MRI) and DWI revealed multiple points of abnormal signal in the pontine, left cerebellum, and bilateral hemispheres, which indicated cerebral embolism (Figure 1). No apparent abnormalities were detected in MRA. However, SWI in the head showed plaque-like low-signal shadows scattered symmetrically throughout the brainstem, bilateral cerebellum, and bilateral hemispheres (Figure 2). An X-ray of the femur revealed a fracture of the left femoral shaft. Combined with the patient's typical clinical manifestations, laboratory tests, and imaging studies, we diagnosed the patient with cerebral fat embolism syndrome. The patient was given neurotrophic, anti-infection, and

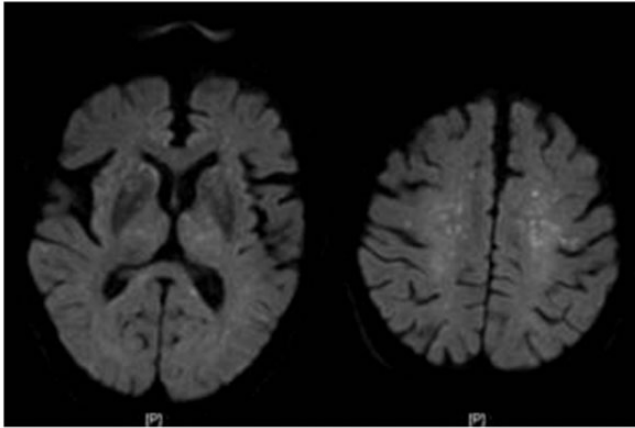


**Figure 1.** Head diffusion-weighted imaging shows multiple punctate diffusion-restricted signals in the bilateral thalamus, corona radiata, and centrum semiovale.

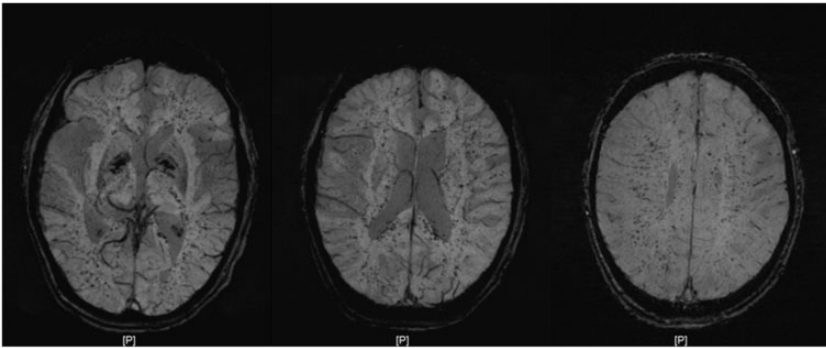


**Figure 2.** Head susceptibility-weighted imaging shows patchy low-signal shadows in the bilateral thalamus, corona radiata, and centrum semiovale, as well as in the bilateral hemispheres.

symptomatic support treatment, and was then gradually weaned from the ventilator and steadily recovered consciousness. Because of the patient's older age, the family refused femoral neck surgery and he was discharged after 6 weeks of hospitalization. After 3 months of follow-up, the patients' neurological symptoms and signs had disappeared.

## Discussion

CFE is a severe complication secondary to long bone fractures, and is rarely observed

in clinical practice. It is a concurrent sign of fat embolism involving the brain.<sup>1</sup> After a long bone fracture, fat particles enter the systemic circulation, and then enter the arterial system through pulmonary blood vessels and the heart (often combined with ventricular septal defects and oval foramen). The fat particles then enter the brain, causing CFE. The pathogenesis of this disease remains unknown; however, the following hypotheses can be considered: 1) pulmonary embolism is often caused by fat embolism, and hypoxemia and respiratory distress caused by pulmonary

embolism might cause brain injury; 2) a fat embolus travels through the heart or pulmonary artery into cerebral blood vessels, causing a microinfarction, similar to cardiogenic cerebral embolism; and 3) because of the inflammatory effects induced by fat particles, the vascular wall permeability increases, leading to vasogenic edema and microhemorrhage.<sup>2,3</sup> Thus, according to our comprehensive analysis, the pathological mechanisms of brain damage caused by fat particles mainly include microembolism, vasogenic edema, and microhemorrhage. The typical clinical manifestations include focal nerve function loss, restlessness, delirium, epilepsy, lethargy, and coma, which can lead to death in severe cases.<sup>4</sup>

The histopathological changes in adipose particles in brain tissue injury underlie the CFE imaging findings. The early diagnosis of CFE is difficult, and this condition is often life-threatening. To date, only a few cases of CFE have been reported,<sup>5</sup> and the typical imaging features of this condition remain lacking. Owing to its non-invasive and simple operation, a head CT is often used in patients with neurological dysfunction. However, despite its sensitivity to bleeding, CT has limited value in the diagnosis of CFE. Previous studies have reported that CFE lesions are diffuse and multifocal because of the small embolized blood vessels, and so a head CT is often negative.<sup>6</sup> A head CT may reveal positive findings in the case of relatively high levels of bleeding with edema; however, in the case of our patient, no characteristic changes were detected in his head CT upon admission. In contrast, MRI has a high diagnostic value for CFE.

T2WI and FLAIR show vasogenic edema around the lesion; nonetheless, because of the limitation of the time of onset, CFE cannot be diagnosed early.<sup>6</sup> DWI is uniquely sensitive to cytotoxic edema and shows diffusion limitation in the early stages of onset, which is valuable

for the early diagnosis of CFE. However, other diseases that cause diffusion limitation, such as cardiogenic cerebral embolism and multiple sclerosis, cannot be excluded using this imaging technique.<sup>7</sup> A previous study reported that the distribution characteristics of typical lesions of CFE under magnetic resonance imaging are as follows: multiple spot-shaped and symmetrically distributed lesions that are mainly localized in the bilateral centrum semiovale, basal ganglia area, corona radiata, watershed areas, brain stem, cerebellum, and corpus callosum.<sup>8</sup> After admission, our patient underwent head MRI, MRA, DWI, and SWI examination. His CT showed no intracranial hemorrhage, while his MRI revealed the presence of multiple patchy abnormal signals in the pons, left cerebellum, and bilateral hemispheres. Those abnormal signals were equal or slightly lower on T1WI, and were high signals on T2WI, FLAIR, and DWI. The distribution of the lesions was in accordance with the typical imaging features of CFE that have been previously reported.<sup>9,10</sup> No significant vascular stenosis was observed in the MRA of our patient, and the possibility of vascular infarction was excluded. The focus distribution of this patient was diffuse and uniform, which differs from the different-sized lesions formed by cardiogenic cerebral embolism, suggesting that the results should be screened for pulmonary circulation. This phenomenon was consistent with the pathogenesis of CFE. In addition, no structural heart defects were detected by ultrasound or the transcranial Doppler bubble test of the heart, and the possibility of cardiogenic cerebral infarction was excluded.

Compared with a previous imaging report of CFE,<sup>10</sup> our patient underwent increased SWI examination. The SWI showed plaque-like low-signal shadows symmetrically scattered in the brainstem, bilateral cerebellum, bilateral thalamus, and bilateral hemispheres. These signals

were displayed differently than those of DWI. Furthermore, compared with traditional MRI sequences, SWI reveals differences in the magnetic sensitivity characteristics between tissues, and shows low signals for blood vessels, microhemorrhage, calcium ion deposition, and iron ion deposition.<sup>11</sup> In the present study, SWI detected bleeding as early as 23 minutes after the onset of symptoms. In addition, this technology is sensitive to the detection of intracerebral microhemorrhagic foci, with a higher detection rate than that of other conventional CT and MRI test sequences.<sup>12</sup> The extensive and diffuse low SWI signal in the brainstem, cerebellum, thalamus, and bilateral cerebral hemispheres of our patient may be ascribed to microhemorrhages, which is consistent with the pathological changes of CFE; however, the specific components need to be further investigated.

The apparent diffusion component is sensitive to vasogenic edema, with a specific value in the diagnosis of CFE, but it also has limitations, such as the onset time. Thus, a comprehensive analysis of MRI (DWI) and SWI has a high diagnostic value in CFE, and SWI is sensitive and specific to CFE lesions, and can be applied as the characteristic imaging indicator of CFE. The main differential diagnoses of the characteristic SWI imaging manifestations from the CFE MRI sequence are as follows: diffuse axonal injury, primary angiitis of the central nervous system (PACNS), and cerebral amyloid angiopathy (CAA). Diffuse axonal injury and CFE both involve a history of trauma, and the distribution and characteristics of their lesions are also similar. However, diffuse axonal injury is usually accompanied by a history of craniocerebral trauma and the lack of an intermediate consciousness period. In the present case, the patient lost consciousness lost after a fall, but no craniocerebral injury was detected. Hence, diffuse axonal degeneration caused by trauma was

excluded. DWI and SWI of PACNS also show imaging findings that are similar to those of CFE. However, the MRA imaging of our patient did not reveal the typical manifestations of PACNS, such as multiple vascular stenosis and aneurysms (bead-like changes). In addition, although we did not administer immunosuppressive therapy (e.g., hormones), the patient's condition gradually improved. Finally, although PANCS can manifest diffusion-limited changes caused by infarction, these are not completely consistent with the diffusion-limited signal, which is "uniformly consistent" in CFE. For these reasons, PACNS was also excluded in our patient. The main manifestation of CAA is multiple intracranial microhemorrhages, and although SWI-like changes similar to CFE are observed, CAA microhemorrhagic lesions are mostly near-cortical or cortical and are predominantly located in posterior regions, rather than having diffuse distribution and involving the corpus callosum. These imaging features are inconsistent with the SWI findings of our patient. In addition, CAA generally does not show similar DWI findings to CFE. Thus, CAA was also excluded in our patient.

In conclusion, SWI combined with DWI has high sensitivity and specificity for the distribution, range, and characteristics of CFE lesions, and these can be used as the characteristic imaging manifestations for the clinical diagnosis of CFE. Hospitals should conduct early DWI and SWI examinations of patients with suspected CFE to avoid a delayed diagnosis, thus saving lives.

### **Declaration of conflicting interest**

The authors declare that there is no conflict of interest.

### **Ethics statement**

The identity of the patient was not mentioned in this case report, and signed patient consent was therefore unnecessary.

## Funding

This research received no specific grant from any funding agency in the public, commercial, or not-for-profit sectors.

## ORCID iDs

Yali Wang  <https://orcid.org/0000-0002-6218-7523>

Jingzhe Han  <https://orcid.org/0000-0002-8719-5079>

## References

1. Suh SI, Seol HY, Seo WK, et al. Cerebral fat embolism: susceptibility-weighted magnetic resonance imaging. *Arch Neurol* 2009; 66: 1170.
2. Satoh H, Kurisu K, Ohtani M, et al. Cerebral fat embolism studied by magnetic resonance imaging, transcranial Doppler sonography, and single photon emission computed tomography: case report. *J Trauma* 1997; 43: 345–348.
3. Kim HJ, Lee JH, Lee CH, et al. Experimental cerebral fat embolism: embolic effects of triolein and oleic acid depicted by MR imaging and electron microscopy. *AJNR Am J Neuroradiol* 2002; 23: 1516–1523.
4. Simon AD, Ulmer JL and Strottmann JM. Contrast-enhanced MR imaging of cerebral fat embolism: case report and review of the literature. *AJNR Am J Neuroradiol* 2003; 24: 97–101.
5. Mijalski C, Lovett A, Mahajan R, et al. Cerebral fat embolism: a case of rapid-onset coma. *Stroke* 2015; 46: e251–e253.
6. Takahashi M, Suzuki R, Osakabe Y, et al. Magnetic resonance imaging findings in cerebral fat embolism: correlation with clinical manifestations. *J Trauma* 1999; 46: 324–327.
7. Rutman AM, Rapp EJ, Hippe DS, et al. T2\*-weighted and diffusion magnetic resonance imaging differentiation of cerebral fat embolism from diffuse axonal injury. *J Comput Assist Tomogr* 2017; 41: 877–883.
8. Parizel PM, Demey HE, Veeckmans G, et al. Early diagnosis of cerebral fat embolism syndrome by diffusion-weighted MRI. *Stroke* 2001; 32: 2942–2944.
9. Huang CK, Huang CY, Li CL, et al. Isolated and early-onset cerebral fat embolism syndrome in a multiply injured patient: A rare case. *BMC Musculoskelet Disord* 2019; 20: 377.
10. Han YT, Tang J, Gao ZQ, et al. Clinical features and neuroimaging findings in patients with cerebral fat embolism. *Chin Med J* 2016; 129: 874–876.
11. Heyn C, Alcaide-Leon P, Bharatha A, et al. Susceptibility-weighted imaging in neurovascular disease. *Top Magn Reson Imaging* 2016; 25: 63–71.
12. Atlas SW and Thulborn KR. MR detection of hyperacute parenchymal hemorrhage of the brain. *AJNR Am J Neuroradiol* 1998; 19: 1471–1477.